

Submesoscale streamers exchange water on the north wall of the Gulf Stream

Jody M. Klymak¹, R. Kipp Shearman², Jonathan Gula³, Craig M. Lee⁴, Eric A. D'Asaro⁴, Leif N. Thomas⁵, Ramsey R. Harcourt⁴, Andrey Y. Shcherbina⁴, Miles A. Sundermeyer⁶, Jeroen Molemaker⁷, and James C. McWilliams⁷

¹University of Victoria, Victoria, British Columbia, Canada

²Oregon State University, Corvallis, Oregon, USA

³Laboratoire de Physique des Océans, Université de Bretagne Occidentale

⁴Applied Physics Laboratory, University of Washington, Seattle,
Washington USA

⁵Stanford University, Stanford, California, USA

⁶University of Massachusetts Dartmouth, Dartmouth, Massachusetts, USA

⁷University of California, Los Angeles, California, USA

November 1, 2015

Abstract

The Gulf Stream is a major conduit of warm surface water from the tropics to the subpolar North Atlantic. Large mesoscale (> 20 km) “rings” often pinch off, but like the Gulf Stream they are resistant to lateral mixing, and retain their properties for a long time. Here we observe and simulate a sub-mesoscale (< 20 km) mechanism by which the Gulf Stream exchanges water with the cold subpolar water to the north. The front exhibits a strong temperature-salinity contrast, with a distinct mode of “mixed” water between the two water masses that is between 2 and 4 km wide. This mass of water is not seen to increase downstream despite there being substantial energy available for mixing. A series of “streamers” detrain some of this water from the Gulf Stream at the crest of meanders. Subpolar water is entrained replacing the mixed water, and helping to resharpen the front. The water mass exchange can account for a northwards flux of salt of $0.8 - 5$ psu m^2s^{-1} , which can be cast as an effective local diffusivity of $O(100 \text{ m}^2\text{s}^{-1})$. This is similar to bulk-scale flux estimates of $1.2 \text{ psu m}^2\text{s}^{-1}$ and supplies fresh water to the Gulf Stream required for the production of 18-degree subtropical mode water.

36 The Gulf Stream (GS) is the western boundary current of the North Atlantic
37 subtropical wind-driven circulation. It separates from Cape Hatteras where
38 it flows eastward into the North Atlantic. As it flows, it loses heat to the
39 atmosphere and by mixing with the cold water in the subpolar gyre to the
40 north. It also becomes fresher, an observation that can only be explained by
41 entrainment of fresh water from the north [1]. As it entrains water, the GS
42 increases its eastward transport by approximately $4 - 8 \times 10^6 \text{ m}^3 \text{s}^{-1}/100 \text{ km}$
43 (Johns et. al.[2]).

44 The GS has a sharp density front, but it also has a sharp temperature and
45 salinity front, as has been demonstrated at the surface from shipboard surveys[3]
46 and satellite images[4]. The sharpness of the front beneath the surface has
47 been less-clear, and requires high-resolution lateral sampling to resolve. It is
48 also known that the front has a sharp potential vorticity gradient[5], and such
49 gradients act as a barrier to lateral mixing[6, 7]. Despite this barrier, property
50 budgets indicate that there is significant exchange across the north wall[1], and
51 that entrainment of fresh water is necessary to create the dynamically important
52 “18-degree water” that fills much of the upper Sargasso Sea.

53 The mechanisms controlling this lateral mixing have not been identified.
54 There are large eddies that periodically pinch off the GS and carry warm water
55 to the north. However, some of these are re-entrained into the GS and do not
56 result in a net exchange. Instead, tracer budgets across the front appear to be
57 dominated by small-scale processes[8]. To date some of the best direct evidence
58 for cross-front exchange consists of the trajectories of density-following floats
59 placed at the north wall [9, 10]. These floats were observed to regularly detrain
60 from the GS, such that of 95 floats, 26 stayed in the GS, 7 were detrained in rings,
61 and 62 were detrained by mechanisms other than rings[10]. Kinematic theories
62 have been examined to explain the detrainment of the floats [11, 12, 13], and
63 the similarity to satellite images of “streamers” of warm water detraining from
64 the Gulf Stream has been noted. However, direct observations of the processes
65 as it occurs at depth have been lacking.

66 Here we present indirect evidence that there is small-scale mixing ($<0.5 \text{ km}$)
67 on the northern cyclonic side of the GS, and that the mixed water periodically
68 peels off the GS in thin (5-10 km wide) “streamers”. In March 2012 we made
69 high-resolution measurements of the north wall of the GS from 66 W to 60 W
70 (Fig. 1), about 850 km east of where the GS separates from the North American
71 continental slope. Two research vessels tracked a water-following float placed in
72 the GS front and programmed to follow the density of the surface mixed layer.
73 The float was transported downstream with a speed of $1.4 \pm 0.2 \text{ m s}^{-1}$, in water
74 that became denser as the surface of the GS cooled. One vessel maintained tight
75 sampling around the float and deployed an undulating profiler to 200 m, making
76 10-km cross sections every 10 km downstream. The second vessel had an
77 undulating profiler making larger 30-km scale sections. Both profilers measured
78 temperature, salinity and pressure, and had approximately 1-km along-track
79 resolution; both ships also measured ocean currents. Fluorescent dye was de-
80 ployed near the floats on some deployments, and measured by the profilers on
81 the ships. By following the float, a focus on the front was maintained as it

82 curved and meandered to the east.

83 During these observations, the GS had a shallow meander crest at 65 W
84 (Fig. 1b) followed by a long concave region (63 W) and then another large crest
85 (61 W). Satellite measurements show the sharp temperature changes across the
86 front, superimposed with thin intermediate-temperature (15-18°C) streamers
87 detraining to the north at approximately 65 W, 64 W, and at the crest of the
88 large meander at 61 W. An older streamer that has rolled up can also be seen at
89 62 W. The ships passed through the three newer streamers providing the first
90 detailed observations of their underwater structure.

91 The front consists of density surfaces that slope up towards the north (Fig. 2a-
92 d). The water along density surfaces is saltier (and warmer) in the GS, and
93 fresher (and colder) to the north. The transition between the two water masses
94 is remarkably abrupt, occurring over less than 5-km. This sharpness per-
95 sisted from our western-most section during the cruise (71.5 W) to the eastern-
96 most (60.5 W). Some cross sections clearly show lateral interleaving of salinity
97 north of the front (Fig. 2a) with approximately 5-km wide salinity anomalies
98 ($S \approx 36.15$ psu). These anomalies move slower than the front (Fig. 2e), and
99 have high potential vorticity that is normally associated with the front (Fig. 2i).

100 The temperature-salinity (T/S) relationship of this data shows the contrast
101 between the GS and the subpolar water as two distinct modes (Fig. 3a), except
102 near the surface where the water masses are strongly affected by the atmosphere.
103 For the deeper water, there is a third distinct population between the two larger
104 modes in T/S space that represents the water in the salinity anomalies, and we
105 have labelled as “streamers”. The distinctness in T/S space of the streamers
106 indicates that after the GS and subpolar waters mixed, the partially mixed water
107 continued to mix, condensing it in T/S space (perfectly mixed water would be
108 a dot).

109 Looking at the GS in plan view (Fig. 3b) we see the mixed water that that
110 makes up the streamers is connected along the length of our observations. The
111 first streamer (64.5 W) is horizontally connected over 100 km, and is about 5
112 km wide, and at least 150 m deep. Where the streamer is the most detached
113 (Fig. 2a) the main front is the sharpest of the 4 cross sections. Downstream
114 of this streamer, the mixed water thins before the eastern meander (60.5 W)
115 where there is a second streamer. Further downstream, the mixed water almost
116 disappears by the last cross-section (59 W).

117 We can quantify the rate of detrainment from the first streamer (64.5 W). It
118 starts on the fast side of the front with water flowing approximately 0.25 m s^{-1}
119 faster than the float (Fig. 2h). Upstream, where it is detached (Fig. 2e), it is
120 flowing almost 0.5 m s^{-1} slower than the float. A 5-km wide and 150-m deep
121 streamer, with a relative velocity of 0.75 m s^{-1} represents a rate of detrainment
122 of over $0.5 \times 10^6 \text{ m}^3 \text{ s}^{-1}$.

123 Concurrently, there is a bolus of fresh water from the north that is enfolded
124 between the streamers and the GS, which we will call an “intrusion”. The
125 entrainment of the intrusion is hard to quantify using the data presented above,
126 because it is drawn from a large pool of water upstream. However, a subsequent
127 survey of the north wall (March 14) included a dye release in this water that was

128 observed to be entrained in an intrusion (Fig. 4a-c). The streamer during this
129 occupation was less pronounced than the one described above, but was clear for
130 a number of passes through the north wall. The dye cloud was quite spread out,
131 but the data show clear interleaving of the intrusion water.

132 High-resolution numerical simulations ($dx \approx 500m$, see Methods) resolve
133 these features and also confirm the entrainment of the fresh intrusion (Fig. 4d-
134 i). Seeding the simulation with Lagrangian particles (see methods) allows us to
135 track the evolution of the streamers and the intrusion as the flow moves down-
136 stream. Before the streamer is formed, the water in the intrusion (magenta
137 contours) is near the surface and the streamer water (green contours) is well
138 within the front (Fig. 4d,g). Downstream (Fig. 4e,h) the fresh water has been
139 subducted to 150 m depth, and the streamer has been pushed north of the front.
140 Both water masses accelerate with the GS (Fig. 4f), but the fresh intrusion ac-
141 celerates more, such that the intrusion is entrained and the streamer slows and is
142 detrain. As in the observations, the streamer occupies an intermediate region
143 in T-S space (Fig. 4i, green contour), and originates in the high-vorticity region
144 of the front. The acceleration of the fresh intrusion relative to the streamer is
145 an important finding of the model, as the fresh water now forms a new sharp
146 T-S front with the warm salty GS, and the mixed streamer water is carried away
147 from the front. The model further shows that the streamers are more prominent
148 on the leading edges of meanders, also clearly seen in satellite images (Fig. 1).

149 There are two major implications of the loss of mixed water to the north.
150 The first is that it helps explain why the front at the north wall of the GS
151 remains so sharp. The T/S distribution clearly indicate that there is mixing
152 because of the separate water-class mode. However we also show that the mixing
153 product is carried away in the streamers. It is striking that it is only the mixed
154 water that is carried away, and not high-salinity GS water (Fig. 3b). This
155 implies a dynamical link that we have not seen explored. Streamers have been
156 observed in surface temperature satellite images and indirectly by subsurface
157 floats[9, 11, 14, 15], and this has led to kinematic models in which particles are
158 displaced from streamlines going around propagating meanders [16, 13, 14]. The
159 observations here add to these models by showing that it is only mixed water
160 that leaves the GS. This co-incidence indicates to us a role for small-scale mixing
161 in producing the destabilizing forces that cause this water to detrain from the
162 north wall. The observations and simulation indicate that the meanders of the
163 GS play an important role in the formation of the streamers.

164 The second implication is that the streamers are a mechanism that can
165 balance large-scale budgets that require significant exchange across the GS[1, 8].
166 Such budgets suggest that this region of the GS loses salinity to the north at a
167 rate of $1.2 \text{ psu } \text{m}^2\text{s}^{-1}$ [1]. Each streamer transports $0.2 - 0.5 \times 10^6 \text{ m}^3\text{s}^{-1}$ of water
168 that is $0.8 - 1 \text{ psu}$ saltier than the water that is entrained. Streamers appear
169 approximately every 100-300 km, associated with meanders, so an estimate of
170 their average transport is $0.8 - 5 \text{ psu } \text{m}^2\text{s}^{-1}$, bracketing the large-scale estimates.
171 Working against a gradient of $1 \text{ psu}/10 \text{ km}$ over 200 m depth, the equivalent
172 lateral diffusivity is $40 - 250 \text{ m}^2\text{s}^{-1}$.

173 Here we have observed a submesoscale lateral stirring process along the

174 north wall of the GS. The T/S front remains persistently sharp, despite small-
175 scale mixing evident from the T/S diagrams, and due to a number of possible
176 processes[17, 18]. The mixed water mass does not accumulate, or it would
177 weaken the sharpness of the front. Here we show that the streamers detrain
178 mixed water, and entrain cold and fresh water toward the north wall, resharpening
179 the temperature-salinity front. Further analysis of the data and models
180 will shed light on the exact mechanism triggering the ejection of water from the
181 front via the streamers.

182 Methods

183 The Lagrangian float[19] was placed in the Gulf Stream front based on a brief
184 cross-stream survey, and programmed to match the density of the surface mixed
185 layer (upper 30 m). The float moved downstream at a mean speed of 1.4 m s^{-1} .
186 The *R/V Knorr* tracked the float and deployed a Chelsea Instruments TriAxus
187 that collected temperature, salinity, and pressure (CTD) on a 200-m deep saw-
188 tooth with approximately 1-km lateral spacing in a 10-km box-shaped pattern
189 relative to the float (Fig. 1, magenta). *R/V Atlantis* performed larger cross
190 sections approximately 30 km across the front, trying to intercept the float on
191 each front crossing. *R/V Atlantis* was deploying a Rolls Royce Marine Mov-
192 ing Vessel Profiler equipped with a CTD that profiled to 200 m approximately
193 every 1 km. Both ships had a 300 kHz RDI Acoustic Doppler Current Pro-
194 filer (ADCP) collecting currents on 2-m vertical scale averaged every 5 minutes
195 (approximately 1 km lateral scale), collected and processed using UHDAS and
196 CODAS (<http://currents.soest.hawaii.edu>[20]). This data reached about 130 m,
197 and was supplemented at deeper depths with data from 75 kHz RDI ADCPs,
198 with 8-m vertical resolution.

199 Data were interpolated onto depth surfaces by creating a two-dimensional
200 interpolation onto a grid via Delauney triangulation. No extrapolation was
201 performed. Data on the 26.25 kg m^{-3} isopycnal were assembled at each grid
202 point by finding the first occurrence of that isopycnal in depth.

203 Potential vorticity is calculated from the three-dimensional grid as

$$q = -\frac{g}{\rho_0} (\nabla \times \mathbf{u} + \mathbf{f}) \cdot \nabla \rho, \quad (1)$$

204 where f is the Coriolis frequency, g the gravitational acceleration. The brack-
205 eted term is twice the angular velocity, including the planet's rotation, and the
206 gradient of density represents the stretching or compression of the water col-
207 umn. In the GS, the potential vorticity is dominated by contributions from
208 the vertical density gradient and the cross-stream gradient of the along-stream
209 velocity:

$$q \approx N^2 \left(-\frac{\partial u}{\partial y} + f \right). \quad (2)$$

210 Dye Release. At select times during the float evolutions, fluorescein dye
211 releases (100 kg per release) were conducted at depth as close as possible to the

212 float. Dye was pumped down a hose to a tow package deployed off the side of
213 the ship, consisting of a CTD and a dye diffuser. Prior to injection, the dye was
214 mixed with alcohol and ambient sea water to bring it to within 0.001 kg m^{-3}
215 of the float's target density. Initial dimensions of the dye streak were $\approx 1 \text{ km}$
216 along-stream, $\approx 100 \text{ m}$ cross-stream (after wake adjustment), and ranging from
217 1 - 5 m in the vertical. The TriAxus system on the *R/V Knorr* tracked the
218 fluorescein from its CTD package.

219 Numerical simulation. The high-resolution realistic simulation of the GS
220 is performed with the Regional Oceanic Modeling System (ROMS[21]). This
221 simulation has a horizontal resolution of 500m and 50 vertical levels. The model
222 domain spans 1,000 km by 800 km and covers a region of the GS downstream
223 from its separation from the U.S. continental slope. Boundary conditions are
224 supplied by a sequence of two lower-resolution simulations that span the entire
225 GS region and the Atlantic basin, respectively. The simulation is forced by
226 daily winds and diurnally modulated surface fluxes. The modelling approach is
227 described in detail in Gula et. al[22].

228 Virtual Lagrangian Particles. Neutrally buoyant Lagrangian (flow-following)
229 particles were seeded at time 285 and advected both backwards and forwards
230 from this time by the model velocity fields without additional dispersion from
231 the model's mixing processes[23]. A 4th-order Runge-Kutta method with a time
232 step $dt = 1 \text{ s}$ is used to compute particle advection. Velocity and tracer fields
233 are interpolated at the positions of the particles using cubic spline interpolation
234 in both the horizontal and vertical directions. We use hourly outputs from the
235 simulation to get sufficiently frequent and temporally-smooth velocity sampling
236 for accurate parcel advection.

237 References

- 238 [1] Joyce, T. M., Thomas, L. N., Dewar, W. K. & Girton, J. B. Eighteen
239 degree water formation within the Gulf Stream during CLIMODE. *Deep*
240 *Sea Res. II* (2013).
- 241 [2] Johns, W., Shay, T., Bane, J. & Watts, D. Gulf Stream structure, trans-
242 port, and recirculation near 68 W. *J. Geophys. Res.* **100**, 817–817 (1995).
- 243 [3] Ford, W., Longard, J. & Banks, R. On the nature, occurrence and origin
244 of cold low salinity water along the edge of the Gulf Stream. *J. Mar. Res.*
245 **11**, 281–293 (1952).
- 246 [4] Churchill, J. H., Cornillon, P. C. & Hamilton, P. Velocity
247 and hydrographic structure of subsurface shelf water at the Gulf
248 Stream's edge. *J. Geophys. Res.* **94**, 10791–10800 (1989). URL
249 <http://dx.doi.org/10.1029/JC094iC08p10791>.
- 250 [5] Rajamony, J., Hebert, D. & Rossby, T. The cross-stream potential vorticity
251 front and its role in meander-induced exchange in the Gulf Stream. *J. Phys.*
252 *Oceanogr.* **31**, 3551–3568 (2001).

- 253 [6] Marshall, J., Shuckburgh, E., Jones, H. & Hill, C. Estimates and implications
254 of surface eddy diffusivity in the Southern Ocean derived from tracer
255 transport. *J. Phys. Oceanogr.* **36**, 1806–1821 (2006).
- 256 [7] Naveira Garabato, A. C., Ferrari, R. & Polzin, K. L. Eddy stirring in the
257 Southern Ocean. *J. Geophys. Res.* **116** (2011).
- 258 [8] Bower, A. S., Rossby, H. T. & Lillibridge, J. L. The Gulf Stream-barrier
259 or blender? *J. Phys. Oceanogr.* **15**, 24–32 (1985).
- 260 [9] Bower, A. & Rossby, T. Evidence of cross-frontal exchange processes in
261 the Gulf Stream based on isopycnal RAFOS float data. *J. Phys. Oceanogr.*
262 **19**, 1177–1190 (1989).
- 263 [10] Bower, A. S. & Lozier, M. S. A closer look at particle exchange in the Gulf
264 Stream. *J. Phys. Oceanogr.* **24**, 1399–1418 (1994).
- 265 [11] Flierl, G., Malanotte-Rizzoli, P. & Zabusky, N. Nonlinear waves and co-
266 herent vortex structures in barotropic β -plane jets. *J. Phys. Oceanogr.* **17**,
267 1408–1438 (1987).
- 268 [12] Stern, M. E. Lateral wave breaking and “shingle” formation in large-scale
269 shear flow. *J. Phys. Oceanogr.* **15**, 1274–1283 (1985).
- 270 [13] Pratt, L. J., Susan Lozier, M. & Beliakova, N. Parcel trajectories in quasi-
271 geostrophic jets: Neutral modes. *J. Phys. Oceanogr.* **25**, 1451–1466 (1995).
- 272 [14] Lozier, M., Pratt, L., Rogerson, A. & Miller, P. Exchange geometry re-
273 vealed by float trajectories in the Gulf Stream. *J. Phys. Oceanogr.* **27**,
274 2327–2341 (1997).
- 275 [15] Song, T., Rossby, T. & Carter, E. Lagrangian studies of fluid exchange
276 between the Gulf Stream and surrounding waters. *J. Phys. Oceanogr.* **25**,
277 46–63 (1995).
- 278 [16] Bower, A. S. A simple kinematic mechanism for mixing fluid parcels across
279 a meandering jet. *J. Phys. Oceanogr.* **21**, 173–180 (1991).
- 280 [17] Thomas, L. N. & Shakespeare, C. A new mechanism for mode water for-
281 mation involving cabbeling and frontogenetic strain at thermohaline fronts.
282 In press *J. Phys. Oceanogr.*
- 283 [18] Whitt, D. B. & Thomas, L. N. Near-inertial waves in strongly baroclinic
284 currents. *J. Phys. Oceanogr.* **43**, 706–725 (2013).
- 285 [19] D’Asaro, E. A. Performance of autonomous Lagrangian floats. *J. Atmos.*
286 *Ocean. Tech.* **20**, 896–911 (2003).
- 287 [20] Firing, E., Hummon, J. M. & Chereskin, T. K. Improving the quality
288 and accessibility of current profile measurements in the Southern Ocean.
289 *Oceanography* (2012).

- ²⁹⁰ [21] Shchepetkin, A. & McWilliams, J. The regional oceanic modeling sys-
²⁹¹ tem (ROMS): a split-explicit, free-surface, topography-following-coordinate
²⁹² oceanic model. *Ocean Modell.* **9**, 347–404 (2005).
- ²⁹³ [22] Gula, J., Molemaker, M. J. & McWilliams, J. C. Gulf Stream dynam-
²⁹⁴ ics along the southeastern US seaboard. *J. Phys. Oceanogr.* **45**, 690–715
²⁹⁵ (2015).
- ²⁹⁶ [23] Gula, J., Molemaker, M. J. & McWilliams, J. C. Submesoscale cold fila-
²⁹⁷ ments in the Gulf Stream. *J. Phys. Oceanogr.* **44**, 2617–2643 (2014).

298 **List of Figures**

- 299 1 **Experimental design.** Inset: The experiment site on the north
300 wall of the Gulf Stream, between 66 and 60 W, as shown in an
301 AVHRR satellite image of sea surface temperature (SST). Main:
302 Detailed SST image composed from two satellite images. The
303 GS is warm and delineated by a sharp front. The small sub-
304 mesoscale structures north of the front are the focus of this paper.
305 The satellite images are a composite from early in the observation
306 period (AVHRR 6 Mar), and late (MODIS, 9 Mar). A Lagrangian
307 float was deployed in the front (black curve), and the ship tracks
308 bracketed the float's position (green: *R/V Atlantis*, magenta:
309 *R/V Knorr*). *R/V Atlantis* cross-sections labeled a-d are shown
310 in Fig. 2a-d. 311 13
- 311 2 **Cross sections of data collected across the Gulf Stream.**
312 Y is the cross-stream distance perpendicular to the path of the
313 float, positive being northwards. The four columns correspond
314 to the four sections labeled a-d in Fig. 1. Potential density is
315 contoured in black and $\sigma_0 = 26.25 \text{ kg m}^{-3}$ is magenta. Along a
316 constant density surface salty water is warmer than fresher water,
317 so the GS on the left is warm and salty. Section a) is the fur-
318thest upstream section (65W) and d) is the furthest downstream
319 (63.75 W) (Fig. 3b). e)-h) downstream velocity calculated rela-
320 tive to the float's trajectory by removing the float's mean speed
321 of $u_{\text{float}} = 1.4 \text{ m s}^{-1}$ for the observation period. Green contours
322 are regions in temperature-salinity space labeled "streamers" in
323 Fig. 3a. i)-l) Potential vorticity (see methods); 324 14

| | |
|-----|---|
| 344 | 4 Evidence for entrainment of intrusions from a dye re- |
| 345 | lease and numerical simulation. a) Salinity section from |
| 346 | an occupation of the GS 14 March. The location of a dye is |
| 347 | contoured in magenta. b) Salinity section from downstream. A |
| 348 | streamer has enfolded the dye in cold-fresh water between itself |
| 349 | and the GS. c) Temperature-salinity diagram for this occupa- |
| 350 | tion. The temperature-salinity for the dye is coloured in dark |
| 351 | magenta. d) Salinity in the GS on the $\sigma_\theta = 26.25 \text{ kg m}^{-3}$ isopyc- |
| 352 | nal from a high-resolution numerical simulation at t_0 . The green |
| 353 | contours delineate the location of particles seeded downstream in |
| 354 | the streamer at time $t_1 = t_0 + 70\text{h}$ (see panels e and h) and ad- |
| 355 | vected <i>backwards</i> in time to t_0 showing where the streamer water |
| 356 | originated. The dark magenta contour is the location of particles |
| 357 | seeded in the fresh intrusion. The straight line shows the location |
| 358 | of the salinity cross-section in panel g. e) as panel d, except at |
| 359 | $t_1 = t_0 + 70\text{ h}$; this is the time and locations where the two clouds |
| 360 | of particles were seeded. g) and h) salinity cross sections for times |
| 361 | t_0 and t_1 . The location of the particles is shown in green and dark |
| 362 | magenta contours. The the $\sigma_\theta = 26.25 \text{ kg m}^{-3}$ isopycnal is con- |
| 363 | toured in light magenta. These panels show that the origin of the |
| 364 | streamer water was in the GS front, and that the fresh-cold water |
| 365 | (magenta contour) enfolded against the front came from north of |
| 366 | the front. f) shows the speeds of the particle clouds in time, and |
| 367 | shows that the intrusion water (magenta) accelerates relative to |
| 368 | the streamer water (green). i) The temperature-salinity of all |
| 369 | the data at t_1 , with the clouds of seeded particles indicated in |
| 370 | T/S space. Note that the green streamer water occupies a mixed |
| 371 | mode between the warm GS waters and the cold and fresh water |
| 372 | to the north. |

16

373 **Acknowledgements** Our thanks to the captains and crews of *R/V Knorr*
374 and *R/V Atlantis*, The AVHRR Oceans Pathfinder SST data were obtained from
375 the Physical Oceanography Distributed Active Archive Center (PO.DAAC) at
376 the NASA Jet Propulsion Laboratory, Pasadena, CA. <http://podaac.jpl.nasa.gov>.
377 The bulk of this work was funded under the Scalable Lateral Mixing and Co-
378 herent Turbulence Departmental Research Initiative and the Physical Oceanog-
379 raphy Program.

380 **Author Contributions** JMK did the main analysis of the data and wrote
381 the paper. JMK, CL, EAD, KS, MS, AS, LT collected the data, performed
382 quality control. RH supplied satellite imagery both at sea and on land. JG,
383 JM and JM ran the simulations and analyzed them. All authors contributed
384 significantly to the analysis and interpretation of these results.

385 **Competing Interests** The authors declare that they have no competing fi-
386 nancial interests.

387 **Correspondence** Correspondence and requests for materials should be ad-
388 dressed to Jody Klymak. (email: jklymak@uvic.ca).

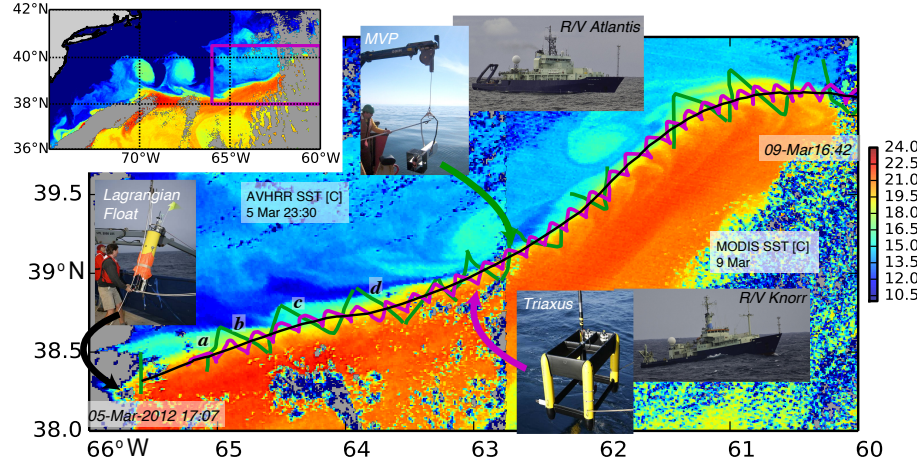


Figure 1: Experimental design. Inset: The experiment site on the north wall of the Gulf Stream, between 66 and 60 W, as shown in an AVHRR satellite image of sea surface temperature (SST). Main: Detailed SST image composed from two satellite images. The GS is warm and delineated by a sharp front. The small sub-mesoscale structures north of the front are the focus of this paper. The satellite images are a composite from early in the observation period (AVHRR 6 Mar), and late (MODIS, 9 Mar). A Lagrangian float was deployed in the front (black curve), and the ship tracks bracketed the float's position (green: *R/V Atlantis*, magenta: *R/V Knorr*). *R/V Atlantis* cross-sections labeled a-d are shown in Fig. 2a-d.

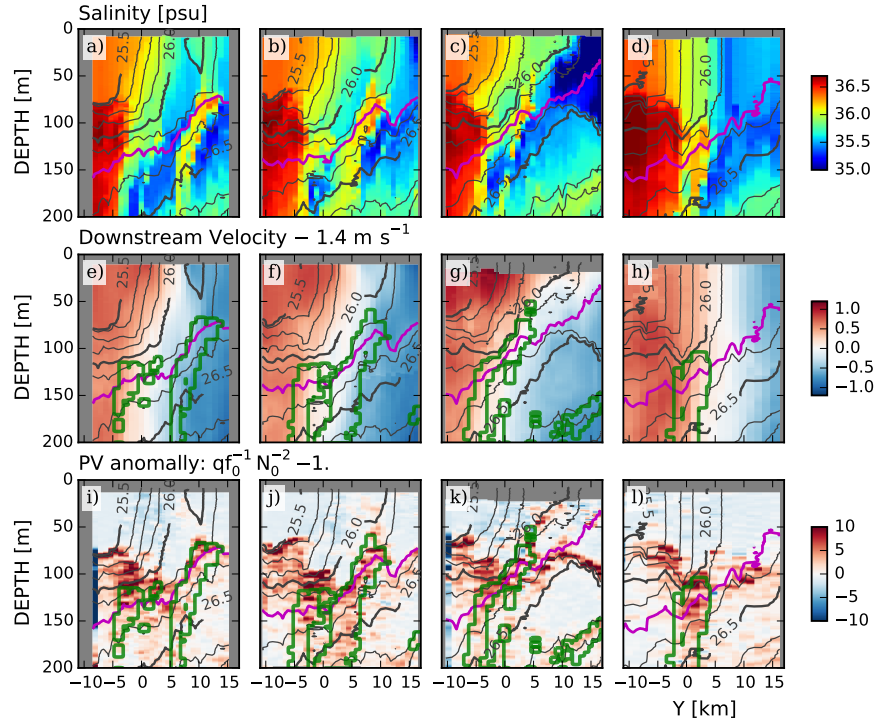


Figure 2: Cross sections of data collected across the Gulf Stream. Y is the cross-stream distance perpendicular to the path of the float, positive being northwards. The four columns correspond to the four sections labeled a-d in Fig. 1. Potential density is contoured in black and $\sigma_\theta = 26.25 \text{ kg m}^{-3}$ is magenta. Along a constant density surface salty water is warmer than fresher water, so the GS on the left is warm and salty. Section a) is the furthest upstream section (65W) and d) is the furthest downstream (63.75 W) (Fig. 3b). e)–h) downstream velocity calculated relative to the float’s trajectory by removing the float’s mean speed of $u_{\text{float}} = 1.4 \text{ m s}^{-1}$ for the observation period. Green contours are regions in temperature-salinity space labeled “streamers” in Fig. 3a. i)–l) Potential vorticity (see methods);

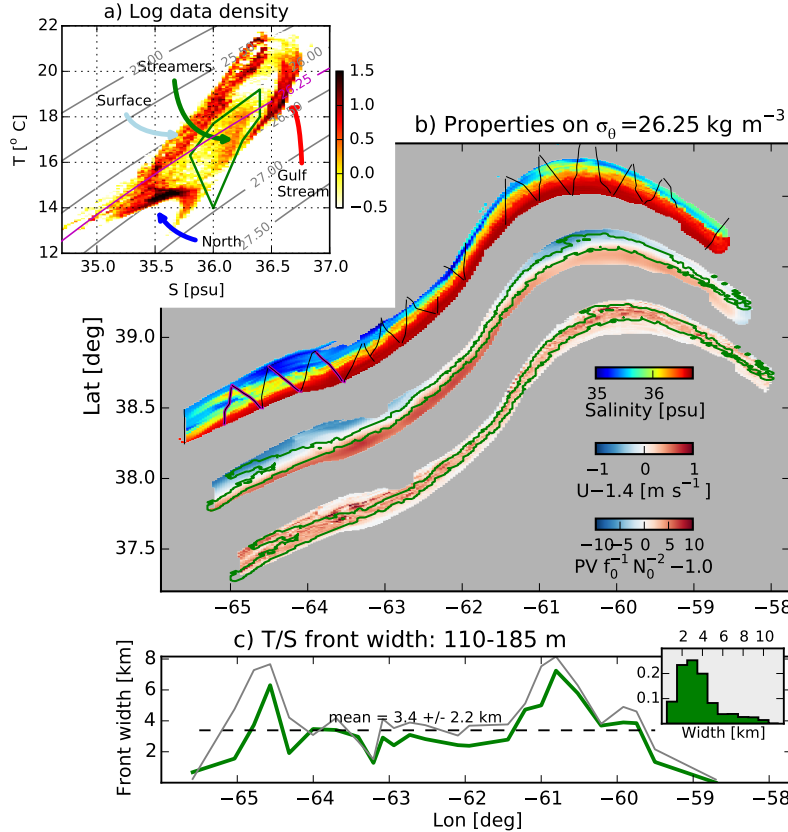


Figure 3: Streamer properties and distribution in space. a) Logarithmically scaled histogram in temperature-salinity space (colours). The warm-salty GS water is distinct from the water to the north, which is cold and fresh. The water near the surface is heavily modified by the atmosphere. Deeper, there is a class of water distinct from the GS water and the water to the north, that we label “streamers”. This water is contoured in green in Fig. 2e-l. b) Interpolation of salinity, velocity, and potential vorticity onto the $\sigma_\theta = 26.25 \text{ kg m}^{-3}$ isopycnal, plotted geographically (with a small exaggeration of scale in the north-south direction, and the latter two fields offset slightly to the south-east). This used data from both ships. The ship track for the *Atlantis* is plotted in black, and the four cross-sections in Fig. 2 are plotted in magenta. The streamer water is contoured in green. c) The width of the T/S front attached to the north wall, averaged between 110 and 185 m (green line). The grey line is the width of all the water in the “streamer” T/S class. A water parcel is considered “attached” if there is no more than one kilometer of water from the fresher water class to the north. This is meant to exclude the clearly detached streamers.

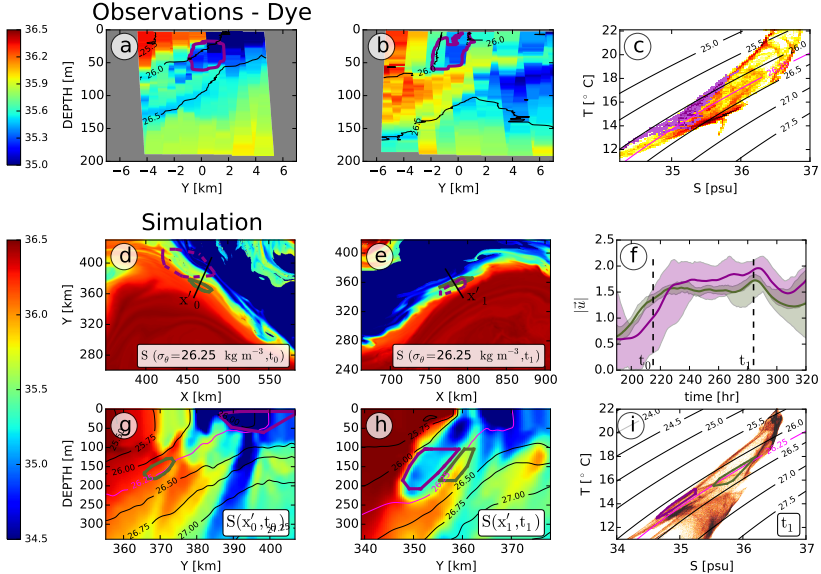


Figure 4: Evidence for entrainment of intrusions from a dye release and numerical simulation. a) Salinity section from an occupation of the GS 14 March. The location of a dye is contoured in magenta. b) Salinity section from downstream. A streamer has enfolded the dye in cold-fresh water between itself and the GS. c) Temperature-salinity diagram for this occupation. The temperature-salinity for the dye is coloured in dark magenta. d) Salinity in the GS on the $\sigma_\theta = 26.25 \text{ kg m}^{-3}$ isopycnal from a high-resolution numerical simulation at t_0 . The green contours delineate the location of particles seeded downstream in the streamer at time $t_1 = t_0 + 70\text{h}$ (see panels e and h) and advected *backwards* in time to t_0 showing where the streamer water originated. The dark magenta contour is the location of particles seeded in the fresh intrusion. The straight line shows the location of the salinity cross-section in panel g. e) as panel d, except at $t_1 = t_0 + 70\text{h}$; this is the time and locations where the two clouds of particles were seeded. g) and h) salinity cross sections for times t_0 and t_1 . The location of the particles is shown in green and dark magenta contours. The the $\sigma_\theta = 26.25 \text{ kg m}^{-3}$ isopycnal is contoured in light magenta. These panels show that the origin of the streamer water was in the GS front, and that the fresh-cold water (magenta contour) enfolded against the front came from north of the front. f) shows the speeds of the particle clouds in time, and shows that the intrusion water (magenta) accelerates relative to the streamer water (green). i) The temperature-salinity of all the data at t_1 , with the clouds of seeded particles indicated in T/S space. Note that the green streamer water occupies a mixed mode between the warm GS waters and the cold and fresh water to the north.